Investigation for Surface Morphology and Mechanical Property Variations of Single Polymer Particles

Dong Ok Kim, Jeong Hee Jin

Advanced Materials Research Division, Hanwha Chemical, 6 Shinsung-Dong, Yusung-Gu, Daejon, 305-804, South Korea

Received 13 August 2006; accepted 1 November 2006
DOI 10.1002/app.25717
Published online in Wiley InterScience (www.interscience.wiley.com).

ABSTRACT: Monodisperse polymer particles were prepared via one-step seeded polymerization using polystyrene, poly(methyl methacrylate), or styrene/methyl methacrylate copolymer [poly(ST-*co*-MMA)] as seed particles and 1,6-hexanedioldiacrylate or divinylbenzene as crosslinking monomer. For the study, the effects of the combination of seed polymer and crosslinking monomer, the ratio of the absorbed monomer to the seed polymer particles (swelling ratio: S/R), and the seeded polymerization rate on the variation of surface morphology and mechanical properties of polymer particles, such as recovery rate, *K*-values, breaking strength, and breaking displacement were investigated by using microcompression test. It was observed that the surface morphology could be controlled by changing polymerization rate or combination of seed polymer and crosslinking monomer, and it had a great influence on mechanical properties, especially the breaking strength. © 2007 Wiley Periodicals, Inc. J Appl Polym Sci 104: 2350–2360, 2007

Key words: polymer particle; swelling ratio; particle structure; surface morphology; mechanical property

INTRODUCTION

In recent years, increased attention has been paid to the development of new electronic packaging technology for making electronic products lighter and smaller, and one of successful examples is the development of anisotropic conductive film technology. Because it can replace conventional soldering and underfill encapsulation processes causing environmental problems and high cost, it is being widely used for packaging technology in flat panel display, such as tape carrier package,[1] chip on glass,[2] or chip on film,[3,4] and is extending its application field to flip chip packaging.[5–10]

ACFs are adhesive films with anisotropic conductivity induced by dispersing conductive particles into polymer matrices such as thermoplastics and thermosetting resins. Mostly metal-coated inorganic or organic particles are used as these conductive particles, and they usually have double layer structure that consists of Ni inner layer for electrical conductivity and Au outer layer for protecting inner layer from the oxidation and increasing the reliability of electrical performance.[11–13]

Correspondence to: D. O. Kim (sky2000cokr@hotmail.com).

Journal of Applied Polymer Science, Vol. 104, 2350–2360 (2007)

However, micron-sized polymer particles with proper mechanical properties (elasticity, hardness, etc.) are preferred as core materials in these days because they can be deformed between bonding electrodes during thermal compression, and this increases the contact area between the bonding electrodes and conductive particles. It is helpful for lowering the connection resistance. Therefore, preparing micron-sized polymer particles having a wide range of mechanical properties is very important.

Traditionally, micron-sized polymer particles have been synthesized by suspension polymerization. However, in spite of the simplicity of suspension polymerization, the size distribution of polymer particles becomes very broad due to the intrinsic nature of suspension polymerization. Thus alternative methods for producing monodisperse micron-sized polymer particles have been developed, including (i) the successive seeding and polymerization due to Vanderhoff et al.,[14] (ii) the activated swelling method due to Ugelstadt and coworkers,[15–17] and (iii) the dynamic swelling method due to Okubo et al.[18,19] About swelling method, one or two steps are needed, i.e., seed polymer particles absorb monomer directly in one-step method but they need to be activated by absorbing a water-insoluble compound such as 1-chlorododecane at first and then absorb monomer in two-steps method. In these methods, because the characteristics of polymerization (e.g., seed polymer, crosslinking monomer, swelling ratio or compati-

TABLE I
Standard Recipe for the Preparation of Poly(ST-*co*-MMA) Seed Polymer Particles by Dispersion Polymerization

Chemicals	Amount (g)
Styrene	46
MMA	20
IPA	400
Water	200
Polyvinylpyrrolidone (K-30)	6
AIBN	2

bility between the monomer and seed polymer) determine the final size, surface morphology, or mechanical properties of the polymer particles, systematic investigation of the relationship between them is very important for the application of polymer particles to core materials of conductive particles. But very little investigation has been reported in the literature except for several patents.[20–22]

In this study, using five mechanical properties (recovery rate, *K*-values, breaking strength, and breaking displacement) that were introduced in patents,[20–22] we investigated the effects of (1) the combination of seed polymer and crosslinking monomer, (2) the ratio of the absorbed monomer to the seed polymer particles, and (3) the seeded polymerization rate on the variation of surface morphology and mechanical properties of polymer particles prepared via one-step seeded polymerization.

EXPERIMENTAL

Materials

For the preparation of seed polymer particles, polystyrene (PS), poly(methyl methacrylate) (PMMA), and poly(ST-*co*-MMA) by dispersion or soap free polymerization, styrene monomer, and MMA (Junsei) were distilled under vacuum and stored in the refrigerator. For the dispersion polymerization, 2,2′-

TABLE II
Physical Properties of Seed Polymer Particles

Seed polymer	D (μm)	C_v	M_W
PS	1.31	5.0	38,000
PMMA	1.30	4.7	43,000
Poly(ST-*co*-MMA)	1.10	5.2	59,000

$C_v(\%) = \sigma/D_n \times 100$ (σ: standard deviation of diameter, D_n: number average diameter).

TABLE III
Ingredients for the Synthesis of Polymer Particles by Seeded Polymerization

Chemicals	Amount (g)
Crosslinking monomer	1
Initiator	0.05
SLS (0.3%) solution	17
PVA (3%) solution	3

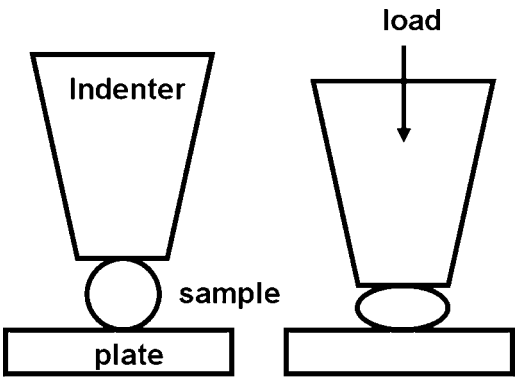

Figure 1 Schematic of the MCT.

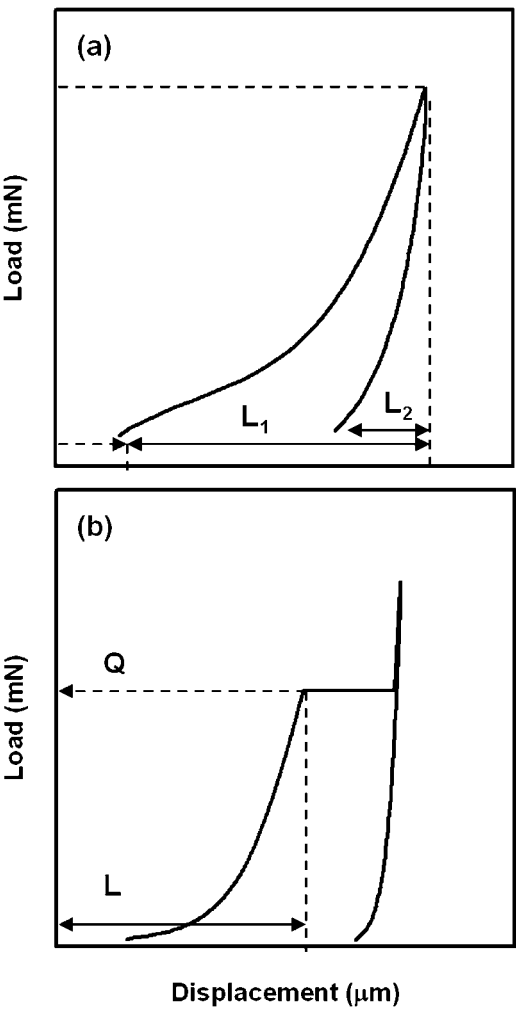

Figure 2 Plots of load versus compression displacement for (a) recovery rate measurement and for (b) *K*-values, breaking strength, and breaking displacement of monodisperse polymer particle.

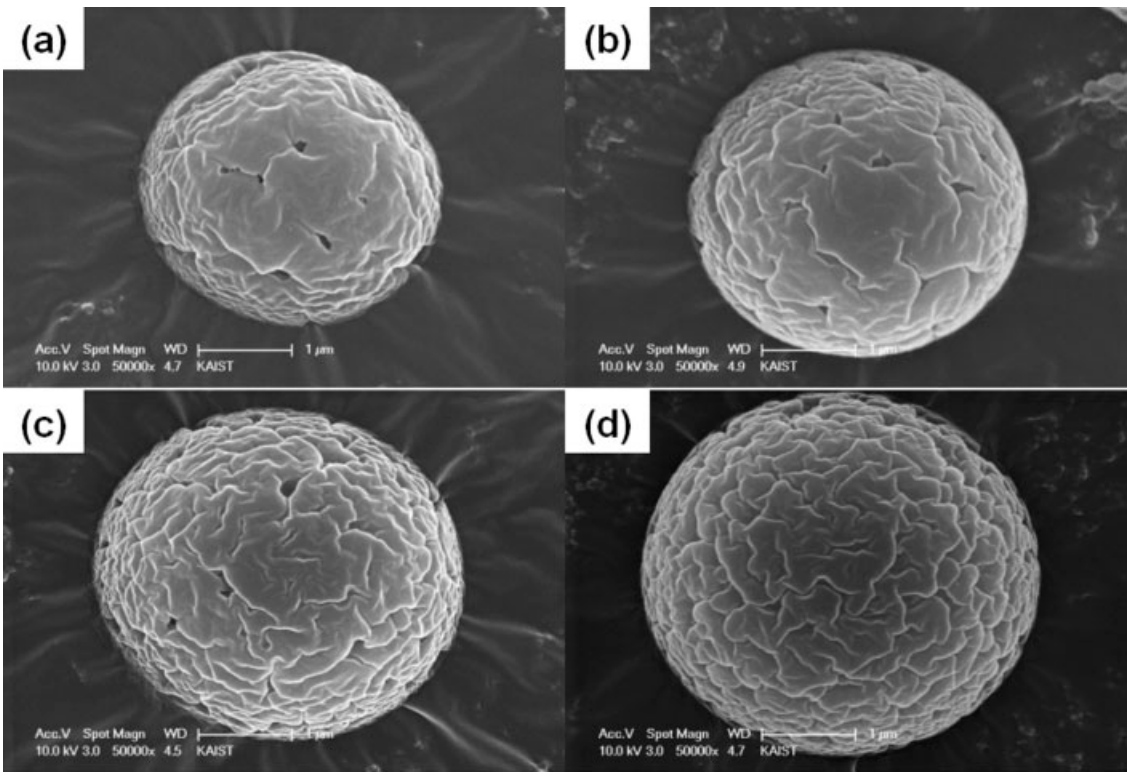

Figure 3 The SEM photographs of the PS/HDDA polymer particles prepared at 70°C with different swelling ratio (S/R) : (a) 20 (C_v : 5.1), (b) 30 (C_v : 5.3), (c) 40 (C_v : 5.3), and (d) 50 (C_v : 5.4).

azobisisobutyronitrile (AIBN) was used as initiator and polyvinyl pyrrolidone (PVP, K-30) was used as dispersant. On the other hand, KPS (potassium persulfate, Junsei) was used as initiator for the soap free polymerization.

For the seeded polymerization, 1,6-hexanedioldiacrylate (HDDA) and divinylbenzene (DVB) were purchased from Aldrich and used as crosslinking monomers without further purification. 2,2′-Azobis(4,4′-dimethylvaleronitrile) (VT-65, Wako), having 6-h half-life temperature at 51°C, was used as initiator. Poly(vinyl alcohol) (PVA, Aldrich), having a weight–average molecular weight of 85,000–146,000, was used as dispersant for polymerization, and sodium-laurylsulfate (SLS, Aldrich) was used as emulsifying agent for emulsification of monomer mixtures.

Polymerizations

The polymerization procedure for the preparation of poly(ST-*co*-MMA) seed particles via dispersion polymerization is as follows.

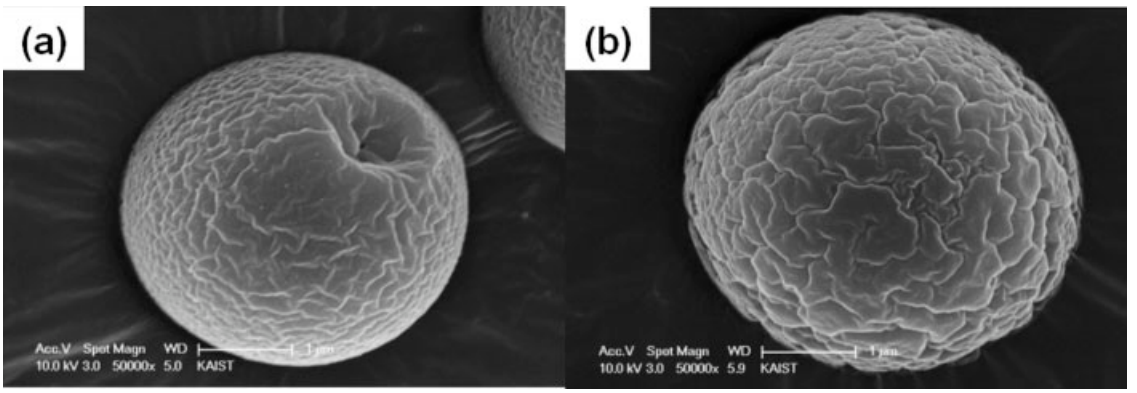

Figure 4 The SEM photographs of the PS/HDDA polymer particles with different polymerization temperature (S/R : 40): (a) 40°C (C_v : 5.5) and (b) 80°C (C_v : 5.4).

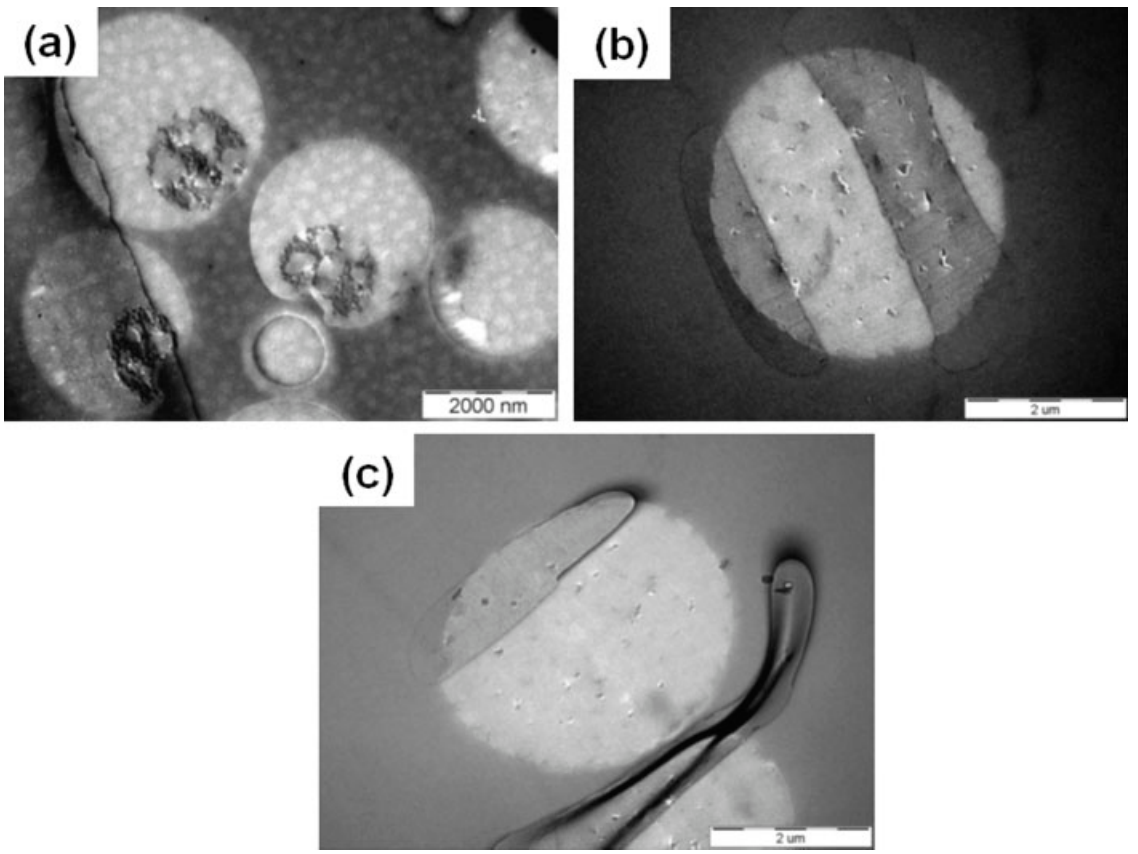

Figure 5 The TEM photographs describing the cross sections of PS/HDDA polymer particles: (a) Figure 3(a), (b) Figure 2(c), and (c) Figure 3(b).

First, the chemicals summarized in Table I were put into a 1000-mL round flask equipped with a mechanical stirrer and reflux condenser under a well controlled temperature. The chemicals were stirred gently with nitrogen purging for 1 h to remove dissolved oxygen. Then, the temperature of the reactor was increased to 70°C and a predetermined amount of initiator was added to the reactor, and the polymerization reaction was continued 12 h. The reactor was cooled down and the seed particles were separated using centrifugation, washed with methanol three times, and dried in a vacuum oven. The details of the synthesis procedures employed for PMMA seed particles are described elsewhere.[23] The characteristics of seed particles thus prepared are summarized in Table II.

For the seeded polymerization, the chemicals summarized in Table III were added to a 50 mL vial and emulsified using ultrasonic homogenizer. A predetermined amount of seed particles was added to above monomer emulsion and this vial was placed in a shaking incubator at room temperature for 24 h for monomer absorption. After the monomer absorption, a predetermined amount of PVA solution was added and polymerization was performed in a shaking bath under temperature control for 24 h. After the polymerization, the same separation and cleaning procedures employed for the seed polymerization were used to collect the polymer particles.

Characterizations and mechanical property measurements

The analysis of polymer particle size and distribution was performed by using AccuSizer™ 780A (PSS.NICOMP, USA). The surface and cross-sectional morphologies of polymer particles were examined by using SEM (JEM 1200EX, Japan) and TEM (ZEISS EM912). The mechanical properties such as recovery rate, *K*-values, breaking strength, and breaking displacement were obtained by calculating the average value of 10 individual particles' MCT (microcompression test, Fisher H100C) measurements. The measurement method for each mechanical property is as follows.

Recovery rate (R_r)

As shown in Figures 1 and 2(a), A polymer particle (diameter: *D*, radius: *R*) is placed on the smooth surface sample table and compressed with indenter

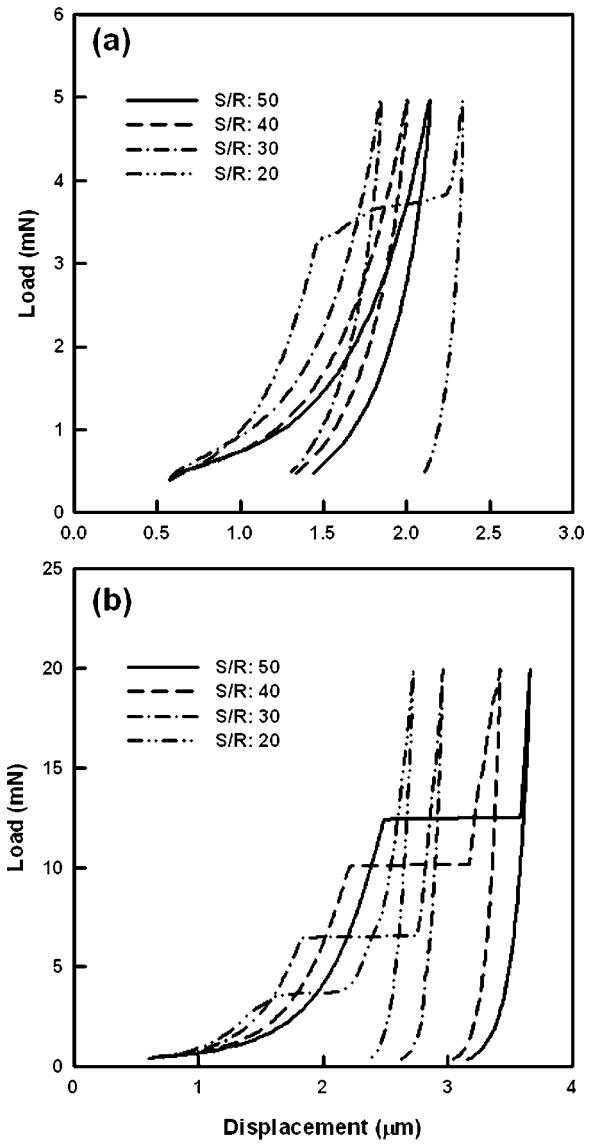

Figure 6 Plots of load versus displacement for (a) recovery rate measurement and for (b) *K*-values, breaking strength, and breaking displacement of PS/HDDA polymer particles with different swelling ratio.

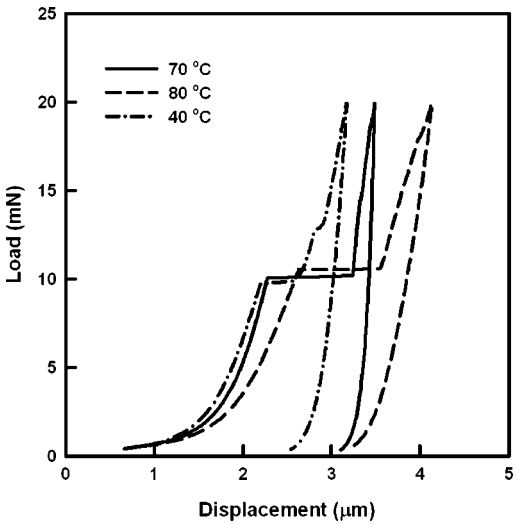

Figure 7 Plots of load versus displacement for mechanical properties measurement of PS/HDDA polymer particles synthesized at different temperatures (*S*/*R* : 40).

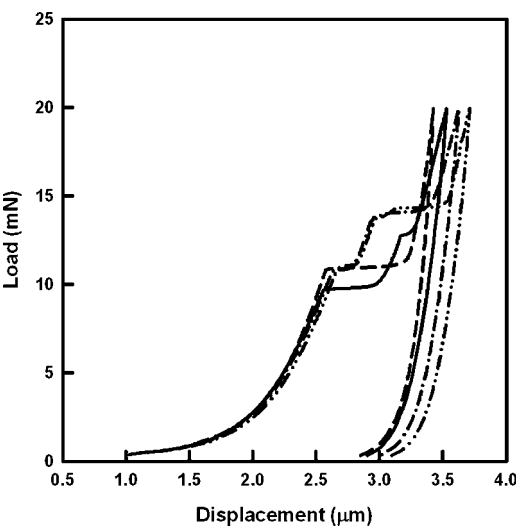

Figure 8 Plots of load versus displacement for mechanical properties measurement of PS/HDDA polymer particles synthesized at 40°C (*S*/*R* : 40).

at the speed of 1 mN/s to maximum load value (5 mN), and after that, the load is decreased at the same speed to standard load value (0.1 mN). The recovery rate represents the degree of particle recoverability after being deformed by compressing, and is defined as the ratio (L_2/L_1) represented by %, wherein L_1 is the displacement from standard load point to maximum load point during compression

TABLE IV
Variation of Mechanical Properties of PS/HDDA Polymer Particles with Different Swelling Ratio

S/R	D_n (μm)	R_r (%)	K_{10} (MPa)	K_{20} (MPa)	S_0 (MPa)	F_r (%)
20	4.19	–	1164	802	141	39
30	4.41	45	1182	876	293	45
40	4.57	51	1362	968	421	50
50	4.61	49	1438	1017	522	54

TABLE V
Variation of Mechanical Properties of PS/HDDA Polymer Particles Synthesized at Different Temperatures (*S*/*R* : 100)

Temp. (°C)	D_n (μm)	R_r (%)	K_{10} (MPa)	K_{20} (MPa)	S_0 (MPa)	F_r (%)
80	4.57	51	1439	1003	462	56
40	4.57	54	831	556	–	–

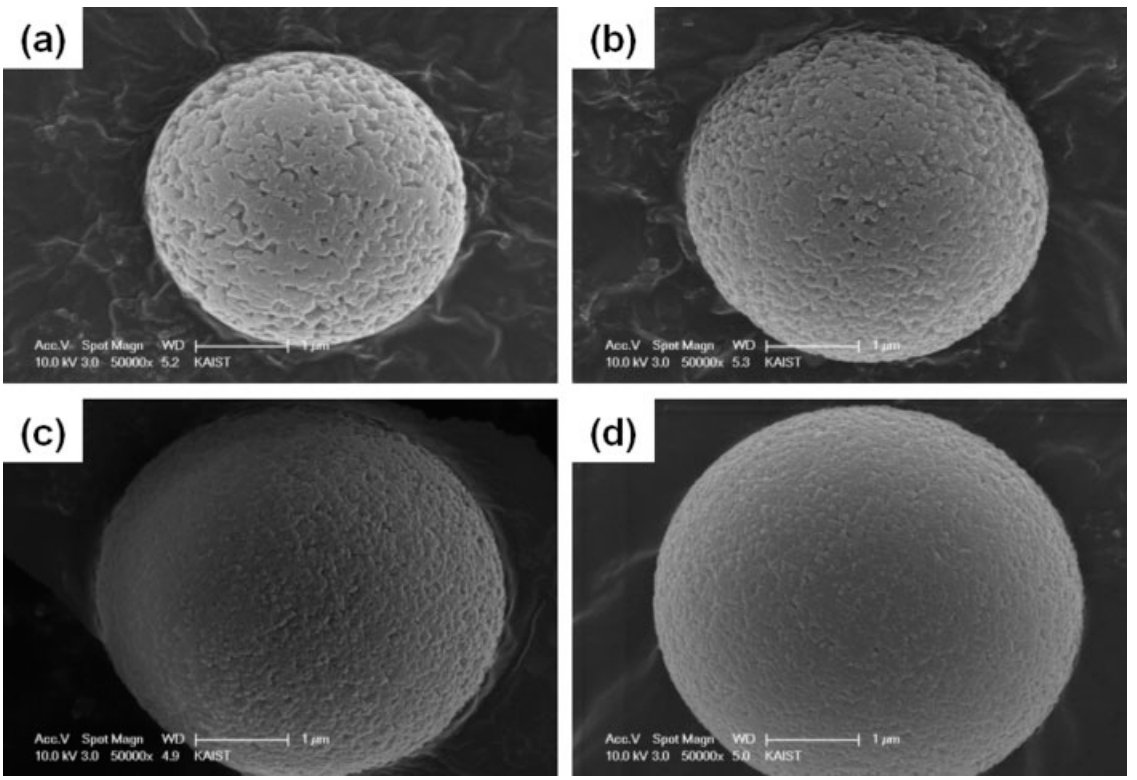

Figure 9 The SEM photographs of the PS/DVB polymer particles prepared at 70°C with different swelling ratio (S/R): (a) 20 (C_v : 5.6), (b) 30 (C_v : 5.8), (c) 40 (C_v : 5.5), and (d) 50 (C_v : 5.6).

and L_2 is the displacement from the maximum load point to the standard load value during releasing.

$$R_r = (L_2/L_1) \times 100 \quad (1)$$

K-values (K_{10} and K_{20})

Load value (F) and compression displacement (S) at the point of 10% (or 20%) compression deformation of the particle are measured while compressing single particle with indenter at the speed of 0.67 mN/s. *K*-values are defined as follows and represent the degree of particle hardness.

$$K = (3/2^{1/2})FS^{-3/2}R^{-1/2} \quad (2)$$

Breaking strength (S_0)

Breaking strength represents the compression rupture strength of the particle. It is calculated by measuring load value (Q) at the breaking point while compressing with indenter at the speed of 0.67 mN/s

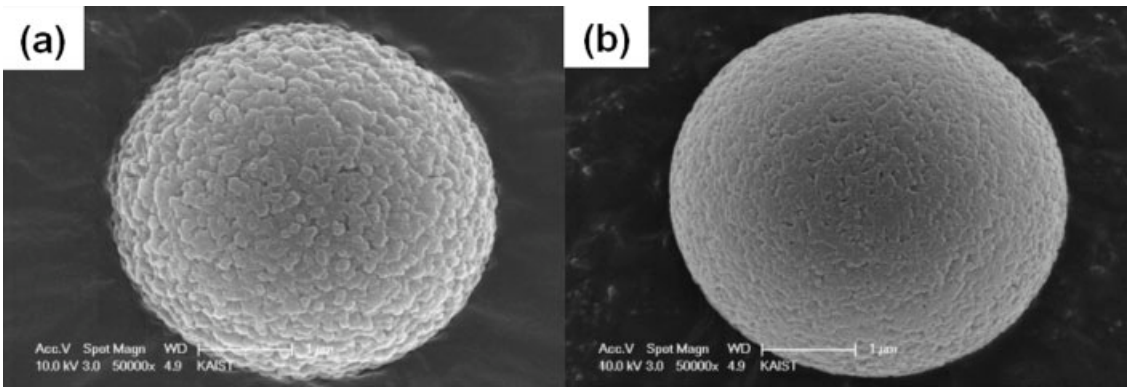

Figure 10 The SEM photographs of the PS/DVB polymer particles with different polymerization temperature (S/R: 40): (a) 20°C (C_v : 5.7) and (b) 80°C (C_v: 5.5).

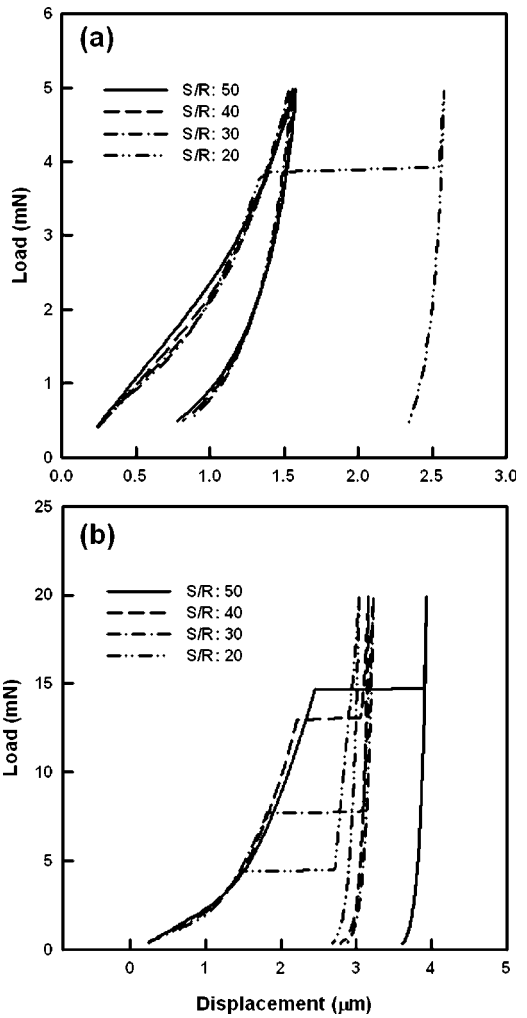

Figure 11 Plots of load versus displacement for (a) recovery rate measurement and for (b) *K*-values, breaking strength, and breaking displacement of PS/DVB polymer particles with different swelling ratio.

as shown in Figure 2(b), and defined as follows.

$$S_0 = 2.8Q/\pi D^2 \quad (3)$$

Breaking displacement (F_r)

Breaking displacement represents the compression rupture displacement of the particle. It is calculated by measuring compression displacement (L) at the breaking point while compressing as shown in Figure 2(b), and defined as the ratio (L/D) represented by %, wherein D is the diameter of particle.

$$F_r = (L/D) \times 100 \quad (4)$$

RESULTS AND DISCUSSION

Effect of crosslinking monomer

In this study, using PS as seed particles, polymer particles having relatively low surface hardness were prepared using HDDA, while polymer particles having relatively high surface hardness were prepared using DVB as crosslinking monomer via one-step seeded polymerization. It is worth noting that using crosslinking monomers having poor compatibility with seed polymers is not usually recommended for seeded polymerization because phase separation occurs during the polymerization. In other words, because DVB has relatively higher compatibility with PS, PS/DVB polymer particles does not show severe phase separation problem, whereas PS/HDDA polymer particles show distinctive phase separation phenomenon, such as crater shaped defect, as shown in the previous study.[24] Polymer particles having such defect are not suitable for the core material of conductive particle because they show very deteriorated mechanical properties. However, using the surface morphology control technology introduced in the previous publication,[24] we solved the phase separation problem of PS/HDDA particles, i.e., changing their surface morphology from crater shaped defect to porous or rough structure, and then observed the variation of mechanical properties.

Figure 3 shows the SEM photographs showing the variation of surface morphology of PS/HDDA polymer particles with swelling ratio. In spite of relatively low swelling ratios, porous structures instead of crater shaped defect were obtained (S/R: 20, 30, and 40) because of relatively fast polymerization rate. But slight difference, i.e., intermediate surface morphology between porous and rough structures, was observed at the swelling ratio of 50. In addition to swelling ratio, the effect of polymerization temperature was also observed by changing the polymerization temperature to 40 and 80°C, and crated shaped defect and rough structure surface morphologies were obtained respectively, (S/R: 40) as shown in Figure 4. The observation of cross-sectional morphologies of polymer particles was also performed to investigate the difference in inside morphologies of polymer particles having three different surface morphologies. It can be seen in Figure 5 that polymer particles having crated shaped defect show large size phase separated domains located near surface, while polymer particles having porous or rough structure surface morphology show small

TABLE VI
Variation of Mechanical Properties of PS/DVB Polymer Particles with Different Swelling Ratio

S/R	D_n (μm)	R_r (%)	K_{10} (MPa)	K_{20} (MPa)	S_0 (MPa)	F_r (%)
20	2.98	–	4937	3645	372	48
30	3.29	56	4637	3636	564	53
40	4.28	57	4138	3268	581	50
50	4.74	59	4204	3296	592	52

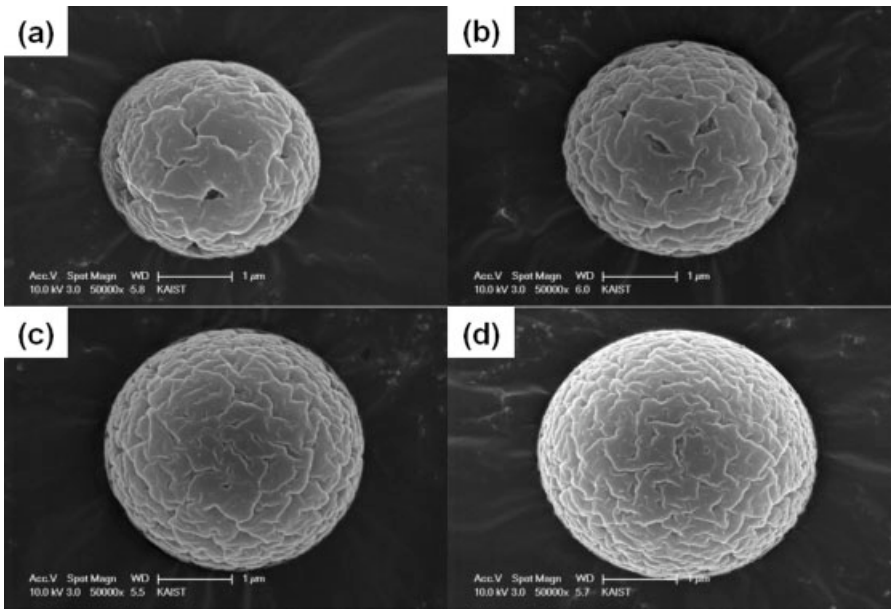

Figure 12 The SEM photographs of the poly(ST-*co*-MMA)/HDDA polymer particles prepared at 70°C with different swelling ratio (S/R) : (a) 20 (C_v : 5.3), (b) 30 (C_v : 5.6), (c) 40 (C_v : 5.6), and (d) 50 (C_v : 5.8).

and well dispersed phase separated domains. However, the size of phase separated domains for rough structure is smaller than that of porous structure particle.

Thus, we confirmed the change of surface morphology with the polymerization rate, and investigated the differences in their mechanical properties. Figure 6(a) shows the MCT results for the measurement of the recovery rate, and Figure 6(b) shows the MCT results for the measurement of the K-values, breaking strength and breaking displacement of PS/HDDA polymer particles with the increase of swelling ratio. Mechanical properties calculated from Figure 6 were summarized in Table IV. It can be seen in Table IV that every mechanical property except recovery rate was increased with swelling ratio. Among them, the degree of increasing for breaking strength was distinctively higher, indicating that breaking strength is closely related to the variation of swelling ratio, i.e., the ratio of crosslinked domain in the polymer particle. On the other hand, the recovery rate was remained more or less constant with the swelling ratio.

For the investigation of the effect of surface morphology change on the mechanical properties, MCT measurement of polymer particles shown in Figure 4 was also performed. Figure 7 shows the MCT measurement result of PS/HDDA polymer particles shown in Figures 3(c) and 4(a,b), and inconsistent MCT measurement results of particles shown in Figure 4(a) were gathered separately in Figure 8. Mechanical properties calculated from Figure 7 were summarized in Table V. As can be seen in Figure 8 and Table V, the measurement of breaking strength

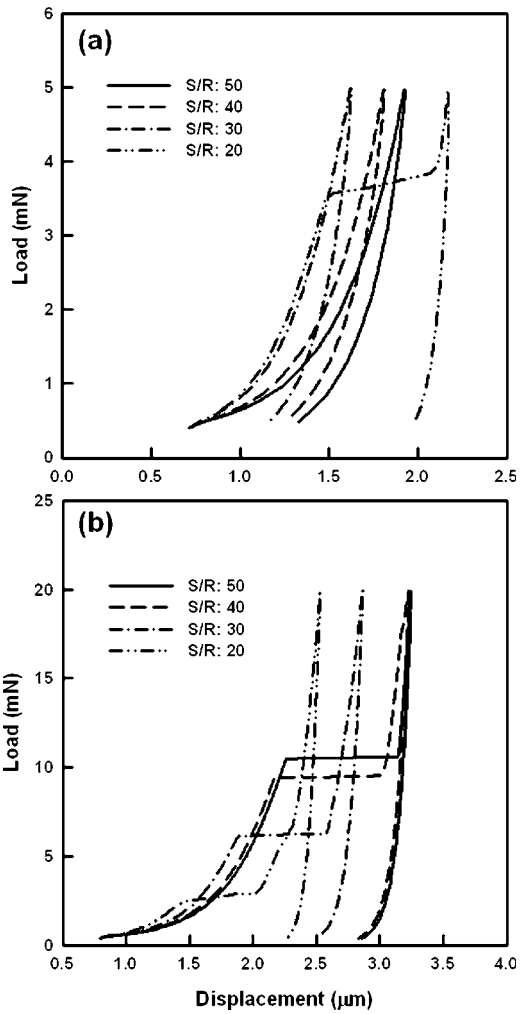

Figure 13 Plots of load versus displacement for (a) recovery rate measurement and for (b) *K*-values, breaking strength, and breaking displacement of poly(ST-*co*-MMA)/HDDA polymer particles with different swelling ratio.

TABLE VII
Variation of Mechanical Properties of Poly(ST-*co*-MMA)/HDDA Polymer Particles with Different Swelling Ratio

S/R	D_n (μm)	R_r (%)	K_{10} (MPa)	K_{20} (MPa)	S_0 (MPa)	F_r (%)
20	3.61	–	1052	718	162	43
30	4.02	55	1181	761	342	48
40	4.28	56	1134	868	481	51
50	4.39	55	1189	884	513	53

and breaking displacement of particles having crater shaped defect was almost impossible due to the lack of consistency, but they were increased as the surface was changed from porous structure [Fig. 3(c)] to rough structure [Fig. 4(b)]. *K*-values were also increased as the surface morphology was changed from crater shaped defect to rough structure. Needless to say, polymer particles having small and well-dispersed phase separated domains have superior mechanical properties to polymer particles having large and poorly dispersed phase separated domains. On the basis of the observations made above, we can conclude that the surface morphology control by increasing polymerization rate is an effective method to increase the mechanical properties of polymer particles showing severe phase separation during polymerization.

Using DVB, PS/DVB polymer particles were also prepared with the increase of swelling ratio and temperature, and then their surface morphologies were observed as shown in Figures 9 and 10. Contrary to PS/HDDA polymer particles, the surface morphology of polymer particles was remained more or less unchanged with the swelling ratio and polymerization temperature, indicating that DVB has higher compatibility with PS seed polymer than HDDA. Figure 11 shows the MCT measurement results of PS/DVB polymer particles shown in Figure 9, and calculated mechanical properties were summarized in Table VI. Interestingly enough, breaking strength and breaking displacement were increased with the swelling ratio as PS/HDDA polymer particles, but *K*-values were decreased. Thus, we can speculate that breaking strength and breaking displacement are closely related to the ratio of crosslinked polymer domain (S/R), whereas *K*-values are closely related to the characteristics of crosslinking monomer.

Effect of seed polymer

In the previous section, HDDA was used as crosslinking monomer for the preparation of polymer particles having relatively low surface hardness. However, phase separation occurred during the

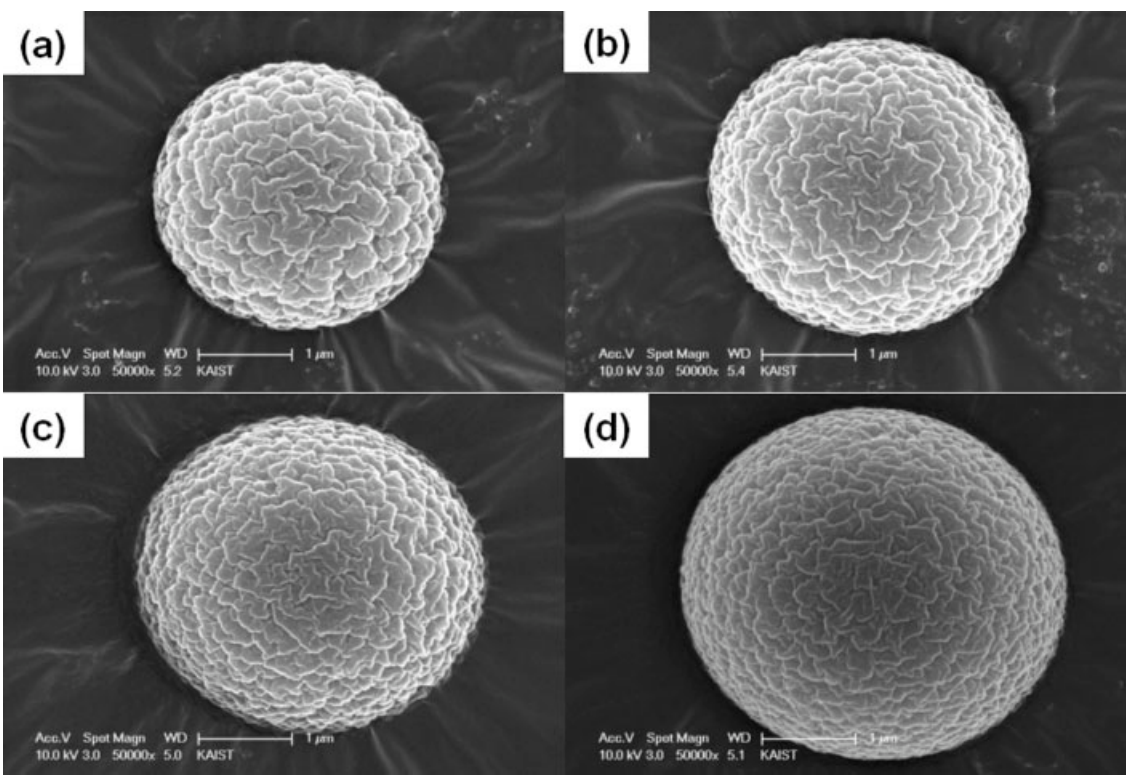

Figure 14 The SEM photographs of the PMMA/HDDA polymer particles prepared at 70°C with different swelling ratio (S/R) : (a) 20 (C_v : 5.8), (b) 30 (C_v : 6.1), (c) 40 (C_v : 5.9), and (d) 50 (C_v : 6.2).

polymerization due to the lack of compatibility, and this gave rise to poor mechanical properties. Thus, the surface morphology control was suggested to overcome the deterioration of mechanical properties.

As an another approach for improving the mechanical properties of PS/HDDA polymer particles, poly(ST-*co*-MMA)/HDDA and PMMA/HDDA polymer particles were prepared using poly(ST-*co*-MMA) and PMMA as seed polymers, and then their mechanical properties were measured. Figure 12 shows SEM photographs describing the surface morphology of poly(ST-*co*-MMA)/HDDA polymer particles with the increase of swelling ratio. Compared with Figure 3, no change in surface morphology was observed at the swelling ratio of 20 and 30, but slight change (i.e., changing from porous to rough structure) was observed at the swelling ratio of 40 and 50, indicating relatively higher compatibility of poly(ST-*co*-MMA) seed polymer. However, MCT measurement

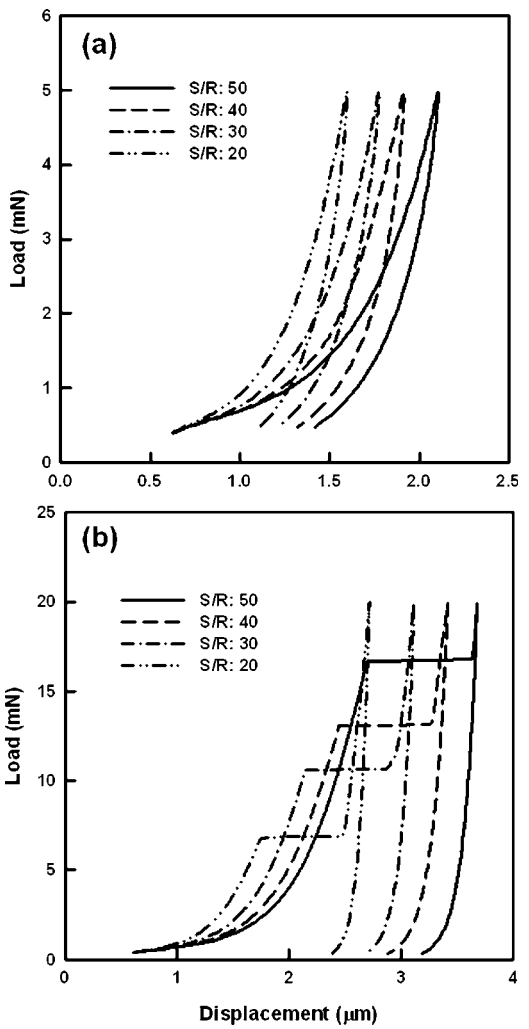

Figure 15 Plots of load versus displacement for (a) recovery rate measurement and for (b) *K*-values, breaking strength, and breaking displacement of PMMA/HDDA polymer particles with different swelling ratio.

TABLE VIII
Variation of Mechanical Properties of PMMA/HDDA Polymer Particles with Different Swelling Ratio

S/R	D_n (μm)	R_r (%)	K_{10} (MPa)	K_{20} (MPa)	S_0 (MPa)	F_r (%)
20	4.0	55	1195	838	363	48
30	4.34	54	1265	938	512	52
40	4.44	51	1330	969	581	55
50	4.47	50	1433	973	783	61

shown in Figure 13 and calculated mechanical properties summarized in Table VII showed very similar results to PS/HDDA polymer particles shown in Figure 6 and Table IV, suggesting that slight difference in surface morphology does not influence the mechanical properties of polymer particles significantly.

As supplementary experiments, a series of polymerizations were repeated using PMMA supposed to have higher compatibility with HDDA than poly (ST-*co*-MMA) as seed polymer. Figure 14 shows the SEM photographs describing the surface morphology of PMMA/MMA polymer particles with the increase of swelling ratio. Contrary to Figures 3 and 12, they showed rough structure surface morphology throughout the entire range of swelling ratio, confirming much higher compatibility of PMMA seed polymer with HDDA. Figure 15 shows the MCT measurement results, and calculated mechanical properties were summarized in Table VIII. *K*-values, breaking strength, and breaking displacement were increased with the swelling ratio, and these behaviors are in good agreement with those of PS/HDDA (Table IV) and poly(ST-*co*-MMA)/HDDA (Table VII). However, breaking strengths of PMMA/HDDA polymer particles at the swelling ratios of 20 and 30 showed much higher values compared with those of PS/HDDA and poly(ST-*co*-MMA)/HDDA particles, indicating that breaking strength is the most sensitive mechanical property to the difference in surface morphology of polymer particles.

CONCLUSIONS

In this study we have observed the variations of surface morphology and mechanical properties of monodisperse polymer particles prepared via one-step seeded polymerization with the combination of seed polymer and crosslinking monomer, swelling ratio, and polymerization rate.

In the case of PS/HDDA polymer particles, although crater shaped defect was observed due to the lack of compatibility, it was changed to the porous or rough structure morphology by increasing polymerization rate. On the other hand, slight change was observed from PS/DVB polymer particles with

the polymerization rate due to the relatively higher compatibility.

When poly(ST-*co*-MMA) particles were used as seed polymer, poly(ST-*co*-MMA)/HDDA polymer particles showed porous structure surface morphology but it changed to rough structure surface morphology as the swelling ratio was increased, whereas PMMA/HDDA polymer particles showed rough structure surface morphology throughout the entire range of swelling ratio, indicating higher compatibility of PMMA seed polymer with HDDA.

The variations of mechanical properties of polymer particles were also investigated. When HDDA was used as crosslinking monomer, every mechanical property except the recovery rate was increased with the increase of swelling ratio, independent of seed polymer. However, when DVB was used, *K*-values was decreased with swelling ratio, leading us to conclude that breaking strength and breaking displacement are closely related to the ratio of crosslinked polymer domain (S/R), while *K*-values are closely related to characteristics of crosslinking monomer. Moreover, it was also observed that the mechanical properties were improved as the surface morphology was changed from crater shaped defect to porous or rough structure. This observation indicated to us that the surface morphology control by changing polymerization rate is an effective method to improve the mechanical properties of polymer particles.

References

1. Watanabe, I.; Fujinawa, T.; Arifuku, M.; Fujii, M.; Gotoh, Y. Presented at the Ninth International Symposium on Advanced Packing Materials, Atlanta, GA, March 24–26, 2004.
2. Joshi, R. Microelectron J 1998, 29, 343.
3. Chang, S.; Jou, J.; Hsieh, A.; Chen, T.; Chang, C.; Wang, Y.; Hung, C. Microelectron Reliab 2001, 41, 2001.
4. Rizvi, M.; Chan, Y.; Sharif, A. Soldering Surf Mount Technol 2005, 17, 40.
5. Sarkar, G.; Mridha, S.; Chong, T.; Yuen, W.; Kwan, S. J Mater Process Technol 1999, 89, 484.
6. Chan, Y.; Luk, D. Microelectron Reliab 2002, 42, 1185.
7. Chan, Y.; Luk, D. Microelectron Reliab 2002, 42, 1195.
8. Wu, Y.; Alam, M.; Chan, Y.; Wu, B. Microelectron Reliab 2004, 44, 295.
9. Seppala, A.; Ristolainen, E. Microelectron Reliab 2004, 44, 639.
10. Uddin, M.; Alam, M.; Chan, Y.; Chan, H. Microelectron Reliab 2004, 44, 505.
11. Goward, J. M.; Whalley, D. C.; Williams, J. Microelectron Int 1995, 37, 55.
12. Whalley, D. C.; Mannan, S. H.; Williams, D. J. Assemb Autom 1997, 17, 66.
13. Oguibe, C. N.; Mannan, S. H.; Whalley, D. C.; Williams, D. J. IEEE Trans Compon Packag Manuf Technol A 1998, 21, 235.
14. Vanderhoff, J. W.; El-Aasser, M. S.; Micale, F. J.; Sudol, E. D.; Tseng, C. D.; Silwanowicz, A.; Kornfeld, D. M.; Vincente, F. A. J Dispersion Sci Technol 1984, 5, 231.
15. Ugelstad, J. Macromol Chem 1978, 179, 815.
16. Ugelstad, J.; Kaggerad, K. H.; Hansen, F. K.; Berge, A. Macromol Chem 1979, 180, 737.
17. Ellinsen, T.; Aune, O.; Ugelstad, J.; Hansen, S. J Chromatogr 1990, 535, 147.
18. Okubo, M.; Shiozaki, M.; Tsujihiro, M.; Tsukuda, Y. Colloid Polym Sci 1991, 269, 222.
19. Okubo, M.; Nakagawa, T. Colloid Polym Sci 1992, 270, 853.
20. Saiuchi, K.; Kohara, H.; Yamada, K.; Kanki, K. U.S. Pat. 5, 486,941 (1996).
21. Saiuchi, K.; Kohara, H.; Yamada, K.; Kanki, K. US Pat 5, 1997, 615, 031.
22. Park, J. K.; Chung, P. M. Korea Pat. 10-2004-002183 (2004).
23. Kim, D. O.; Jin, J. H.; Shon, W. I.; Oh, S. H. J Appl Polym Sci, to appear.
24. Kim, D. O.; Jin, J. H.; Oh, S. H. J Appl Polym Sci, to appear.